Payame Noor University

Control and Optimization in Applied Mathematics (COAM)
Vol. 7, No. 1, Winter-Spring 2022 (1-14), ©2016 Payame Noor University, Iran
DOI. 10.30473/coam.2022.63671.1199 (Cited this article)

Research Article

Applying Robust Adaptive Lyapunov-Based Control for Hexa-Rotor

Mohammad Reza Zarrabi*
Department of Applied Mathematics, School of Mathematics and Computer Science, Damghan University, Damghan.

Received: April 15, 2022; **Accepted:** July 16, 2022.

Abstract. Drones are among the most valuable and versatile technologies in the world, with applications in a vast number of fields such as traffic control, agriculture, firefighting and rescue, and filmmaking, to name a few. As the development of unmanned aerial vehicles (UAVs) accelerates, the safety of UAVs becomes increasingly important. In this paper, a robust adaptive controller is designed to improve the safety of a hexa-rotor UAV, and a robust adaptive controller is developed to control our system. In doing so, the wind parameters from the aerodynamic forces and moments acting on the hexa-rotor are estimated using an observer with the adaptive algorithm. This proposed controller guarantees stability and reliable function in the midst of parametric and non-parametric uncertainties. The process's global stability and tracking convergence are investigated using the Lyapunov theorem. The performance and effectiveness of the proposed controller are tested through two simulation studies, which take into account external disturbances that are a function of time.

Keywords. Hexa-rotor, Adaptive control, Lyapunov function, Adaptive law, Trajectory tracking.

MSC. 45D05; 42C10; 65G99.

* Corresponding author
mzarrabi@du.ac.ir
http://mathco.journals.pnu.ac.ir

1 Introduction

Unmanned Aerial Vehicles (UAVs) have shown great promise in recent years due to their advantages in power and speed over quad-rotors. Various studies have shown that the proper positioning of the rotors is crucial to the success of a hexa-rotor UAV [8], [10] and [13]; other advantages show up in the form of more lift and more time in flight [2], [6] and [15]. The hexa-rotor UAV has significant advantages over other types of UAVs due to its fault tolerance, greater load capacity, and higher stability. This makes it an ideal choice for completing more complex tasks. Therefore, understanding how to control a hexa-rotor UAV is of great importance [9].

To control the hexa-rotor automatically, various control methods have been employed, such as linearization of input and output feedbacks [19], backstepping control [16], sliding mode control (SMC) [3], fuzzy control and other intelligent control methods [11], [14] and [17].

The hexa-rotor's dynamics are significantly influenced by outside disturbances. In order to mitigate this problem, Mokhtari, et al. developed a sliding mode disturbance observer [7]. It is clear that this controller is not robust to wind disturbances that affect the dynamic model of forces and displacement (x, y). In this work, the adaptive technique is applied to the trajectory tracking problem following the structure of [12], but the wind parameters resulting from the aerodynamic forces and moments, which are time-dependent functions, are considered.

Against this backdrop, these wind parameters are estimated using an adaptive observer based on an adaptive control algorithm to ensure convergence within a limited time, thereby providing robustness to external disturbances and variations in parameters for the overall system.

In this paper, we present a new robust adaptive Lyapunov-based controller for the hexa-rotor by combining nonlinear adaptive control and sliding-mode control.

This paper is organized as follows. Section 2 provides a brief overview of the hexa-rotor mathematical model. Section 3 discusses the proposed controller design in detail. Section 4 analyzes the Lyapunov stability of the system. Section 5 presents two examples to illustrate the efficacy of the proposed controller design. Finally, Section 6 offers conclusions and future research directions.

2 Mathematical Model of the Hexa-Rotor

The hexa-rotor is shown in Figure 1. The hexa-rotor consists of six rotors generating F_i $(i = 1, 2, \ldots, 6)$ forces, each of which is attached to a propeller. The six rotors are arranged in two parts, each pointing in opposite directions (Figure 1). Forward motion is achieved by increasing the speed of the rotors $(3, 4, 5)$ while decreasing the same value for the rotors $(1, 2, 6)$. For the movement to the left, the speed of rotors $(5, 6)$ is increased while the speed of rotors $(2, 3)$ is decreased. Other movements can be performed in a similar way [1].

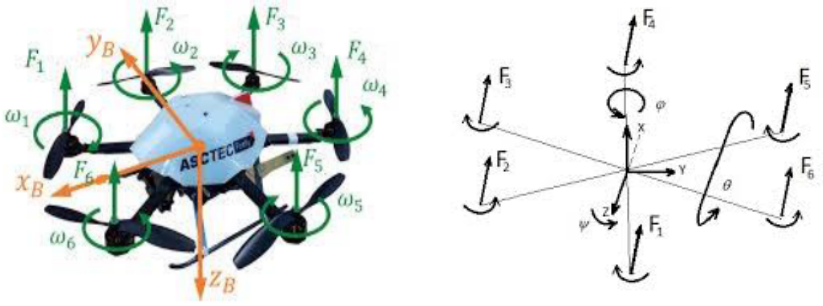

Figure 1: Hexa-rotor aircraft.

The dynamic model of the hexa-rotor consists of the body-frame (x_b, y_b, z_b) and the earth-frame (x_e, y_e, z_e). Let $[x, y, z]'$, $[u, v, w]'$, $[p, q, r]'$, m_s, g, l denote the position of the center of gravity, the hexa-rotor in the earth-frame, the linear velocity in the earth-frame, the angular velocity in the body-frame, the total mass of the aircraft, the acceleration due to gravity, and the distance from the center of each rotor to the center of gravity, respectively.

The orientation of the hexa-rotor is given by the rotation matrix $R(\phi, \theta, \psi)$ shown in Figure 2, as follows:

$$R(\phi, \theta, \psi) = R(z, \psi) \cdot R(y, \theta) \cdot R(x, \phi),$$

where R depends on the three Euler angles $[\phi, \theta, \psi]'$, representing roll, pitch and yaw, respectively. These angles are bounded as follows: roll angle, ϕ, by $\left(-\frac{\pi}{2} < \phi < \frac{\pi}{2}\right)$; pitch angle, θ, by $\left(-\frac{\pi}{2} < \theta < \frac{\pi}{2}\right)$; and yaw angle, ψ, by $(-\pi < \psi < \pi)$. The rotation of the hexa-rotor's body must be compensated for during position control. The compensation is achieved by transposing the rotation matrix where [4],

$$R(z, \psi) = \begin{bmatrix} \cos\psi & -\sin\psi & 0 \\ \sin\psi & \cos\psi & 0 \\ 0 & 0 & 1 \end{bmatrix}, \tag{1}$$

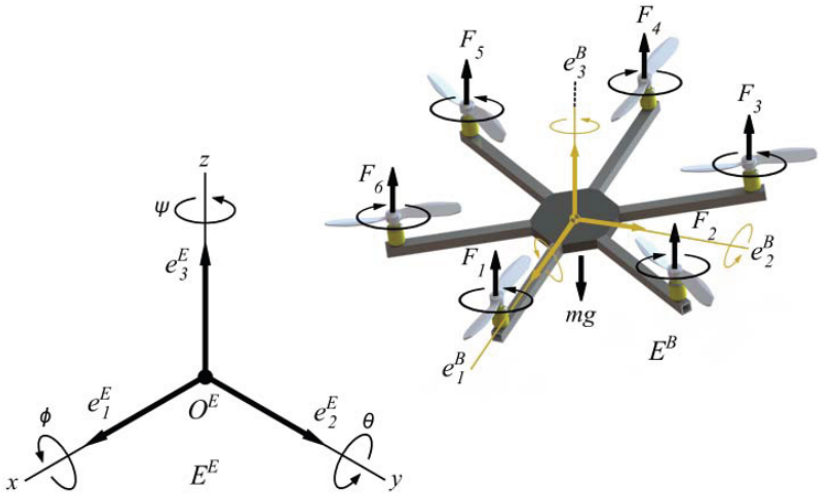

Figure 2: Orientation of the hexa-rotor by using Euler angles.

$$R(y,\theta)=\begin{bmatrix}\cos\theta & 0 & \sin\theta\\ 0 & 1 & 0\\ -\sin\theta & 0 & \cos\theta\end{bmatrix}, \tag{2}$$

$$R(x,\phi)=\begin{bmatrix}1 & 0 & 0\\ 0 & \cos\phi & -\sin\phi\\ 0 & \sin\phi & \cos\phi\end{bmatrix}. \tag{3}$$

Hence,

$$R(\Theta)=R(\phi,\theta,\psi)=\begin{bmatrix}C_\psi C_\theta & C_\psi S_\theta S_\phi - S_\psi C_\phi & C_\psi S_\theta C_\phi + S_\psi S_\phi\\ S_\psi C_\theta & S_\psi S_\theta S_\phi + C_\psi C_\phi & S_\psi S_\theta C_\phi - C_\psi S_\phi\\ -S_\theta & C_\theta S_\phi & C_\theta C_\phi\end{bmatrix}, \tag{4}$$

where $C_{(\cdot)}$ and $S_{(\cdot)}$ represent $\cos(\cdot)$ and $\sin(\cdot)$, respectively.

Kinematics of a rigid body is given by [17]

$$v_e = Rv_b, \tag{5}$$

where $v_e=[u_0,v_0,w_0]'$ and $v_b=[u_b,v_b,w_b]'$ are linear velocities of the center of mass expressed in the earth-frame and the body-frame, respectively.

The matrix of the rotational velocities is [8]

$$M(\Theta)=M(\phi,\theta,\psi)=\begin{bmatrix}1 & 0 & -S_\theta\\ 0 & C_\phi & C_\theta S_\phi\\ 0 & -S_\phi & C_\theta C_\phi\end{bmatrix}. \tag{6}$$

To transfer the angular velocities from the earth-frame to the body-frame, the angular velocity vector in the earth-frame must be matrix multiplied by the inverse of the rotational velocity matrix as follows:

$$\begin{pmatrix}\dot{\phi}\\ \dot{\theta}\\ \dot{\psi}\end{pmatrix} = M^{-1}(\phi,\theta,\psi)\begin{pmatrix}p\\ q\\ r\end{pmatrix} = \begin{pmatrix}1 & S_\phi T_\theta & C_\phi T_\theta\\ 0 & C_\phi & -S_\phi\\ 0 & \frac{S_\phi}{C_\theta} & \frac{C_\phi}{C_\theta}\end{pmatrix}\begin{pmatrix}p\\ q\\ r\end{pmatrix}, \tag{7}$$

where $T_{(\cdot)}$ represents $\tan(\cdot)$.

The translational motion can be described as [11]:

$$m\begin{pmatrix}\ddot{x}\\ \ddot{y}\\ \ddot{z}\end{pmatrix} = -\begin{pmatrix}0\\ 0\\ gm\end{pmatrix} + R_{i,3}U_1 + \begin{pmatrix}K_1\dot{x}\\ K_2\dot{y}\\ K_3\dot{z}\end{pmatrix}, \tag{8}$$

where U_1 is the main control input in the z-axis direction, $R_{i,3}$ is the third column of the translational matrix and $(K_1\dot{x}, K_2\dot{y}, K_3\dot{z})'$ is the air drag vector, distributed in the x_e, y_e and z_e axes, respectively. By considering

$$(D_1, D_2, D_3)' = \frac{1}{m}(K_1\dot{x}, K_2\dot{y}, K_3\dot{z})', \tag{9}$$

and according to Eqs. (4), (8)-(9) the dynamical equations describing the translational dynamics of the hexa-rotor can be written as follows:

$$\begin{cases}\ddot{x} = \frac{1}{m}(C\phi S\theta C\psi + S\phi S\psi)U_1 + D_1,\\ \ddot{y} = \frac{1}{m}(C\phi S\theta C\psi - S\phi C\psi)U_1 + D_2,\\ \ddot{z} = \frac{1}{m}(C\phi C\theta)U_1 - g + D_3,\end{cases} \tag{10}$$

where

$$U_1 = (F_1 + F_2 + F_3 + F_4 + F_5 + F_6), \tag{11}$$

$$F_i = b\Omega_i^2, \tag{12}$$

in which F_i represents the thrust generated by rotor i for $i = 1, 2, \ldots, 6$ and $b > 0$ is the lift coefficient and Ω_i is the angular velocity of the six rotors.

The rolling, pitching and yawing torques represented by M_ϕ, M_θ and M_ψ, respectively, can be expressed as [5] and [9]:

$$M_\phi = \frac{1}{2}db(\Omega_1^2 + \Omega_5^2 + \Omega_6^2 - \Omega_2^2 - \Omega_3^2 - \Omega_4^2), \tag{13}$$

$$M_\theta = \frac{\sqrt{3}}{2}bd(\Omega_4^2 + \Omega_5^2 - \Omega_1^2 - \Omega_2^2), \tag{14}$$

$$M_\psi = l(\Omega_1^2 + \Omega_2^2 + \Omega_3^2 - \Omega_4^2 - \Omega_5^2 - \Omega_6^2), \tag{15}$$

where d and l are the distance between the center of the rotors on the diagonal and the reverse torque coefficient, respectively. In Eq. (13) $\cos 60^\circ = \frac{1}{2}$ represents the torque component of the rotors on the x-axis in the body-frame, and in Eq. (14) $\sin 60^\circ = \frac{\sqrt{3}}{2}$ represents the torque component of the rotors on the y-axis in the body-frame.

The torque balance of the hexa-rotor UAV can be expressed by the Newton–Euler formula as follows [18]:

$$\begin{pmatrix} \dot{p} \\ \dot{q} \\ \dot{r} \end{pmatrix} = I_{xyz}^{-1} \left(- \begin{pmatrix} p \\ q \\ r \end{pmatrix} \times \begin{pmatrix} I_x p \\ I_y q \\ I_z r \end{pmatrix} + \begin{pmatrix} J_R \Omega p \\ J_R \Omega q \\ 0 \end{pmatrix} + \begin{pmatrix} M_\phi \\ M_\theta \\ M_\psi \end{pmatrix} + T_{aero} \right), \tag{16}$$

where $I_{xyz} = \begin{pmatrix} I_x & 0 & 0 \\ 0 & I_y & 0 \\ 0 & 0 & I_z \end{pmatrix}$ and J_R are the inertia matrix and the rotor inertia, respectively. T_{aero} is the UAV system and

$$\Omega = \Omega_1 + \Omega_2 - \Omega_3 + \Omega_4 - \Omega_5 + \Omega_6.$$

In summary, the rotational model of a hexa-rotor UAV can be expressed as:
Rotational dynamics:

$$\begin{cases} \ddot{\phi} = \dot{\theta}\dot{\psi}\dfrac{I_y - I_z}{I_x} + \dfrac{J_R}{I_x}\dot{\theta}w + \dfrac{d}{I_x}U_2 + D_4, \\ \ddot{\theta} = \dot{\phi}\dot{\psi}\dfrac{I_z - I_x}{I_y} + \dfrac{J_R}{I_y}\dot{\phi}w + \dfrac{d}{I_y}U_3 + D_5, \\ \ddot{\psi} = \dot{\phi}\dot{\theta}\dfrac{I_x - I_y}{I_z} + \dfrac{1}{I_z}U_4 + D_6, \end{cases} \tag{17}$$

where

$$\begin{aligned} U_2 &= \frac{\sqrt{3}}{2}(F_4 + F_5 - F_1 + F_2), \\ U_3 &= \frac{1}{2}(F_1 + F_5 + F_6 - F_2 - F_3 - F_4), \\ U_4 &= F_1 + F_2 + F_3 - F_4 - F_5 - F_6, \\ \begin{bmatrix} D_4 \\ D_5 \\ D_6 \end{bmatrix} &= I_{xyz}^{-1} T_{aero}. \end{aligned}$$

3 Design of a Robust Adaptive Controller

The dynamic nonlinear mathematical model can describe the system in its state space of the hexa-rotor with state vector $X = (x_1, x_2, \ldots, x_{12})'$. To design an adaptive controller, substitute

$$\begin{aligned} &x_1 = \phi, \quad x_3 = \theta, \quad x_5 = \psi, \quad x_7 = z, \quad x_9 = x, \quad x_{11} = y, \\ &x_2 = \dot{\phi}, \quad x_4 = \dot{\theta}, \quad x_6 = \dot{\psi}, \quad x_8 = \dot{z}, \quad x_{10} = \dot{x}, \quad x_{12} = \dot{y}. \end{aligned}$$

the Equations (10) and (17) can be rewritten as follows:

$$\begin{cases} \dot{x}_1 = x_2, \\ \dot{x}_2 = a_1 x_4 x_6 + a_2 w x_4 + b_1 U_2 + D_4, \\ \dot{x}_3 = x_4, \\ \dot{x}_4 = a_3 x_2 x_6 + a_4 w x_2 + b_2 U_3 + D_5, \\ \dot{x}_5 = x_6, \\ \dot{x}_6 = a_5 x_2 x_4 + b_3 U_4 + D_6, \\ \dot{x}_7 = x_8, \\ \dot{x}_8 = -g + \frac{1}{m}(\cos x_1 \cos x_3) U_1 D_3, \\ \dot{x}_9 = x_{10}, \\ \dot{x}_{11} = x_{12}, \\ \dot{x}_{12} = \frac{1}{m}(\cos x_1 \sin x_3 \sin x_5 - \sin x_1 \cos x_5) U_1 + D_1, \end{cases} \tag{18}$$

where U_i's are the control inputs to achieve the desired objectives, a_i and b_j are the known constants given by:

$$\begin{aligned} &a_1 = \frac{I_y - I_z}{I_x}, \quad a_2 = -\frac{J_R}{I_x}, \quad a_3 = \frac{I_z - I_x}{I_y}, \quad a_4 = \frac{J_R}{I_y}, \quad a_5 = \frac{I_x - I_y}{I_z}, \\ &b_1 = \frac{d}{I_x}, \quad b_2 = \frac{d}{I_y}, \quad b_3 = \frac{1}{I_z}. \end{aligned}$$

Accordingly, the six arbitrary disturbance functions D_i's are considered as unstructured uncertainties of the hexa-rotor model.
Some of the equations from the dynamics of the hexa-rotor model (18) can be arranged as follows:

$$\begin{cases} U_1 = \dfrac{m(\dot{x}_B + g)}{\cos x_1 \cos x_3} - D_3, \\ U_2 = \dfrac{1}{b_1}(\dot{x}_2 - a_1 x_4 x_6 - a_2 w x_2) - D_4, \\ U_3 = \dfrac{1}{b_2}(\dot{x}_4 - a_3 x_2 x_6 - a_4 w x_2) - D_5, \\ U_4 = \dfrac{1}{b_3}(\dot{x}_6 - a_5 x_2 x_4) - D_6. \end{cases} \tag{19}$$

Using

$$\Gamma_2 = \dot{x}_{2d} - \eta_2(x_2 - x_{2d}), \qquad \Gamma_4 = \dot{x}_{4d} - \eta_4(x_4 - x_{4d}),$$
$$\Gamma_6 = \dot{x}_{6d} - \eta_6(x_6 - x_{6d}), \qquad \Gamma_8 = \dot{x}_{8d} - \eta_8(x_8 - x_{8d}) + g,$$

the regressor matrices Z_j in terms of certain functions of the variables Γ_i's and x_i's and θ_j's are defined in terms of the unknown parameters of dynamical systems (19) (for $j = 1, 2, 3, 4$ and $i = 2, 4, 6, 8$) as follows:

$$Z_1 = \left(\frac{\Gamma_8}{\cos x_1 \cos x_3}\right), \quad Z_2 = (\Gamma_2, x_4 x_6, x_4), \quad Z_3 = (\Gamma_4, x_2 x_6, x_2), \quad Z_4 = (\Gamma_6, x_2 x_4),$$
$$\theta_1 = (m), \quad \theta_2 = \left(\frac{1}{b_1}, -\frac{a_1}{b_1}, -\frac{a_2 w}{b_1}\right), \quad \theta_3 = \left(\frac{1}{b_2}, -\frac{a_3}{b_2}, -\frac{a_4 w}{b_2}\right), \quad \theta_4 = \left(\frac{1}{b_3}, -\frac{a_5}{b_3}\right),$$

where $\tilde{x}_i = x_i - x_{id}$, x_{id} is the desired trajectory, and γ_i's are positive constants. If $x_i \to x_{id}$ then $\Gamma_i \to \dot{x}_i$ for $2, 4, 6$ and 8, so the control law (19) can be reformulated as:

$$\begin{cases} U_1 = Z_1 \hat{\theta}_1 - \dfrac{\gamma_1 \operatorname{sgn}(\tilde{x}_8)}{\cos x_1 \cos x_3}, \\ U_2 = Z_2 \hat{\theta}_2 - \gamma_2 \operatorname{sgn}(\tilde{x}_2), \\ U_3 = Z_3 \hat{\theta}_3 - \gamma_3 \operatorname{sgn}(\tilde{x}_4), \\ U_4 = Z_4 \hat{\theta}_4 - \gamma_4 \operatorname{sgn}(\tilde{x}_6), \end{cases} \tag{20}$$

where " ˆ " is used to indicate the estimated values of the uncertain system parameters, which are updated using adaptation laws.

4 Convergence of the Method

We obtain the dynamics of the closed-loop system using the proposed nonlinear robust adaptive controller by substituting the control laws (20) into the hexa-rotor model (19), and by adding and subtracting some expiration, we obtain

$$\frac{1}{b_1}(\dot{x}_2 - a_1 x_4 x_6 - a_2 w x_2) - D_4 = Z_2 \hat{\theta}_2 - \gamma_2 \operatorname{sgn}(\tilde{x}_2) = \frac{\dot{x}_{2d} - \eta_2(x_2 - x_{2d})}{\hat{b}_1} -$$

$$\frac{\hat{a}_1}{\hat{b}_1}x_2x_6 - \frac{\hat{a}_2\hat{w}}{\hat{b}_1}x_2x_6 - \frac{\hat{a}_2\hat{w}}{\hat{b}_1}x_4 \pm \frac{\dot{x}_{2d} - \eta_2(x_2 - x_{2d})}{b_1}$$
$$\frac{1}{b_2}(\dot{x}_4 - a_3x_2x_6 - a_4wx_2) - D_5 = Z_3\hat{\theta}_3 - \gamma_3\mathrm{sgn}(\tilde{x}_4) = \frac{\dot{x}_{4d} - \eta_4(x_4 - x_{4d})}{\hat{b}_2} -$$
$$\frac{\hat{a}_3}{\hat{b}_2}x_2x_6 - \frac{\hat{a}_4\hat{w}}{\hat{b}_2}x_2 \pm \frac{\dot{x}_{4d} - \eta_4(x_4 - x_{4d})}{b_2}$$
$$\frac{1}{b_3}(\dot{x}_6 - a_5x_2x_4) - D_6 = Z_4\hat{\theta}_4 - \gamma_4\mathrm{sgn}(\tilde{x}_6) = \frac{\dot{x}_{6d} - \eta_6(x_6 - x_{6d})}{\hat{b}_3} - \frac{\hat{a}_5}{\hat{b}_3}x_2x_4 \pm$$
$$\frac{\dot{x}_{6d} - \eta_6(x_6 - x_{6d})}{b_3}\frac{m(\dot{x}_8 + g)}{\cos x_1 \cos x_3} - D_3 = Z_1\hat{\theta}_1 - \frac{\gamma_1\mathrm{sgn}(\tilde{x}_8)}{\cos x_1 \cos x_3} =$$
$$\frac{\dot{x}_{8d} - \eta_8(x_8 - x_{8d}) + g}{\cos x_1 \cos x_3}\hat{m} - \frac{\gamma_1\mathrm{sgn}(\tilde{x}_8)}{\cos x_1 \cos x_3} \pm \frac{m(\dot{x}_{8d} + g - \eta_8\tilde{x}_8)}{\cos x_1 \cos x_3}.$$

By simplification, the dynamics of the closed-loop system are finally expressed as follows:

$$\begin{cases} \dot{\tilde{x}}_2 = -\eta_2\tilde{x}_2 + b_1Z_2\tilde{\theta}_2 - b_1\gamma_2\mathrm{sgn}(\tilde{x}_2) + b_1D_4, \\ \dot{\tilde{x}}_4 = -\eta_4\tilde{x}_4 + b_2Z_3\tilde{\theta}_3 - b_2\gamma_3\mathrm{sgn}(\tilde{x}_4) + b_2D_5, \\ \dot{\tilde{x}}_6 = -\eta_6\tilde{x}_6 + b_3Z_4\tilde{\theta}_4 - b_3\gamma_4\mathrm{sgn}(\tilde{x}_6) + b_3D_6, \\ \dot{\tilde{x}}_8 = -\eta_8\tilde{x}_8 + \frac{1}{m}(\cos x_1 \cos x_3Z_1\tilde{\theta}_1 - \gamma_1\mathrm{sgn}(\tilde{x}_8) + \cos x_1 \cos x_3D_3), \end{cases} \tag{21}$$

where $\tilde{\theta}_i = \hat{\theta}_i - \theta_i$ for $i = 1, 2, 3, 4$ are the vectors of parameter estimation errors.

Theorem 1. If the adaptation laws are defined as:

$$\begin{cases} \dot{\hat{\theta}}_1 = -A_3^TZ_1^T \cos x_1 \cos x_3\tilde{x}_8, \\ \dot{\hat{\theta}}_2 = -A_4^TZ_2^T\tilde{x}_2, \\ \dot{\hat{\theta}}_3 = -A_5^TZ_3^T\tilde{x}_4, \\ \dot{\hat{\theta}}_4 = -A_6^TZ_4^T\tilde{x}_6, \end{cases} \tag{22}$$

if $t \to \infty$ then $x_{2i} \to x_{2id}$ on the condition $\gamma_i \geq |A_{i+2}|$ for $i = 1, 2, 3, 4$.

Proof. To prove the stability of the process and the convergence of the tracking with the proposed controller, a Lyapunov function candidate is used as follows:

$$V = \frac{1}{2}(\Sigma_{i=1}^4(\tilde{x}_{2i})^2 + \tilde{\theta}_1^TA_3^{-1}\tilde{\theta}_1 + b_1\tilde{\theta}_2^TA_4^{-1}\tilde{\theta}_2 + b_2\tilde{\theta}_3^TA_5^{-1}\tilde{\theta}_3 + b_3\tilde{\theta}_4^TA_6^{-1}\tilde{\theta}_4). \tag{23}$$

The time derivative of V is then obtained as follows:

$$\dot{V} = \sum_{i=1}^4 \tilde{x}_{2i}\dot{\tilde{x}}_{2i} + \dot{\tilde{\theta}}_1^TA_3^{-1}\tilde{\theta}_1 + b_1\dot{\tilde{\theta}}_2^TA_4^{-1}\tilde{\theta}_2 + b_2\dot{\tilde{\theta}}_3^TA_5^{-1}\tilde{\theta}_3 + b_3\dot{\tilde{\theta}}_4^TA_6^{-1}\tilde{\theta}_4, \tag{24}$$

where $\dot{\tilde{\theta}}_i = \dot{\hat{\theta}}_i$, because θ_i is a constant vector and $\dot{\theta}_i = 0$. By employing the nonlinear closed-loop dynamics (21) into (24), and considering the adaptation laws (22) we have

$$\begin{aligned}\dot{V} = &\frac{1}{2}(\tilde{x}_2(-\eta_2\tilde{x}_2 + b_1 Z_2\tilde{\theta}_2 - b_1\gamma_2 sgn(\tilde{x}_2) + b_1 D_4) + \tilde{x}_4(-\eta_4\tilde{x}_4 + b_2 Z_3\tilde{\theta}_3 \\ &- b_2\gamma_3 sgn(\tilde{x}_4) + b_2 D_5) + \tilde{x}_6(-\eta_6\tilde{x}_6 + b_3 Z_4\tilde{\theta}_4 - b_3\gamma_4 sgn(\tilde{x}_6) + b_3 D_6) + \tilde{x}_8(-\eta_8\tilde{x}_8 \\ &+ \frac{1}{m}(\cos x_1 \cos x_3 Z_1\tilde{\theta}_1 - \gamma_1 sgn(\tilde{x}_8) + \cos x_1 \cos x_3 D_3)) \\ &+ \frac{1}{m}(-A_3^T Z_1^T \cos x_1 \cos x_3\tilde{x}_8)^T A_3^{-1}\tilde{\theta}_1 + b_1(-A_4^T Z_2^T\tilde{x}_2)^T A_4^{-1}\tilde{\theta}_2 + b_2(-A_5^T Z_3^T\tilde{x}_4)^T A_5^{-1}\tilde{\theta}_3 \\ &+ b_3(-A_6^T Z_4^T\tilde{x}_6)^T A_6^{-1}\tilde{\theta}_4) = \frac{1}{2}((-\eta_2\tilde{x}_2^2 - \eta_4\tilde{x}_4^2 - \eta_6\tilde{x}_6^2 - \eta_8\tilde{x}_8^2) - b_1(\gamma_2 sgn(\tilde{x}_2) - D_4)\tilde{x}_2 \\ &- b_2(\gamma_3 sgn(\tilde{x}_4) - D_5)\tilde{x}_4 - b_3(\gamma_4 sgn(\tilde{x}_6) - D_6)\tilde{x}_6 - \frac{1}{m}(\gamma_1 sgn(\tilde{x}_8) - \cos x_1 \cos x_3 D_3)\tilde{x}_8) \\ \leq &\ 0.\end{aligned}$$

If $\tilde{x}_{2i} > 0$ for $i = 1, 2, 3$ then,

$$\begin{aligned}&sgn(\tilde{x}_{2i}) = 1 \xrightarrow{\gamma_i \geq |D_{i+2}|} (\gamma_{2i} sgn(\tilde{x}_{2i} - D_{2i+2})\tilde{x}_{2i} \geq 0 \\ &\Rightarrow -b_i(\gamma_{2i} sgn(\tilde{x}_{2i}) - D_{2i+2})\tilde{x}_{2i} \leq 0,\end{aligned}$$

and if $\tilde{x}_{2i} < 0$ for $i = 1, 2, 3$ then,

$$\begin{aligned}&sgn(\tilde{x}_{2i}) = -1 \xrightarrow{\gamma_i \geq |D_{i+2}|} (\gamma_{2i} sgn(\tilde{x}_{2i} - D_{2i+2})\tilde{x}_{2i} \geq 0 \\ &\Rightarrow -b_i(\gamma_{2i} sgn(\tilde{x}_{2i}) - D_{2i+2})\tilde{x}_{2i} \leq 0.\end{aligned}$$

Similarly, if $\tilde{x}_8 > 0$ then,

$$\begin{aligned}&sgn(\tilde{x}_8) = 1 \xrightarrow{\gamma_1 \geq |D_3|} (\gamma_1 sgn(\tilde{x}_8) - \cos x_1 \cos x_3 D_3)\tilde{x}_8 \geq 0 \\ &\Rightarrow -\frac{1}{m}(\gamma_1 sgn(\tilde{x}_8) - \cos x_1 \cos x_3 D_3)\tilde{x}_8 \leq 0,\end{aligned}$$

and if $\tilde{x}_8 < 0$ then,

$$\begin{aligned}&sgn(\tilde{x}_8) = -1 \xrightarrow{\gamma_1 \geq |D_3|} (\gamma_1 sgn(\tilde{x}_8) - \cos x_1 \cos x_3 D_3)\tilde{x}_8 \geq 0 \\ &\Rightarrow -\frac{1}{m}(\gamma_1 sgn(\tilde{x}_8) - \cos x_1 \cos x_3 D_3)\tilde{x}_8 \leq 0.\end{aligned}$$

The proposed nonlinear control method guarantees stability and tracking convergence based on the Lyapunov stability theorem. □

5 Simulation Results

Example 1. To probe the estimator, consider perturbations as follows:

$$D_1 = 0.05 * \cos(0.1t), \quad D_2 = 0.01\sin(t), \quad D_3 = 0.02\cos(t),$$
$$D_4 = 1 + 0.5\sin(0.2t), \quad D_5 = 0.2 + 0.1\sin(0.2t), \quad D_6 = 0.4 + 0.2\sin(0.2t),$$

and constant coefficients as follows:

$$a_1 = -a_3 = -1, \quad a_2 = -a_4 = -0.00155, \quad a_5 = 0,$$
$$b_1 = b_2 = 13.89, \quad b_3 = 23.14, \quad w = 0.5, \quad m = 1.830, \quad g = 9.81,$$

and also consider the desirable trajectories as follows:

$$x_{2d} = 0.1e^{-t}, \quad x_{4d} = 0.01e^{-2t}, \quad x_{6d} = e^{-0.01t}, \quad x_{8d} = 0.5e^{-2t},$$

with the following initial data:

$$(x_1, x_2, x_3, x_4, x_5, x_6) = (0.1, 0.5, 0.15, 0.2, -0.05),$$
$$(x_7, x_8, x_9, x_{10}, x_{11}, x_{12}) = (100, -0.05, 50, 0.005, 150, 0.01),$$
$$\theta_1 = 1.8, \quad \theta_2 = (0.1, -0.09, 0.0005), \quad \theta_3 = (0.1, -0.09, -0.0005),$$
$$\theta_4 = (0.04, -0.004).$$

Finally, by applying the adaptive control described in this article, the trajectory of the roll, pitch, and yaw angles and the trajectory of the hexa-rotor position are shown respectively in Figure 3.

Example 2. To probe the estimator, consider perturbations as follows:

$$D_1 = 0.05 * e^{-4t^2}, \quad D_2 = 0.01\sin(t), \quad D_3 = e^{-5t^2},$$
$$D_4 = -e^{-6t^2}, \quad D_5 = 0.2 + 0.1\sin(0.2t), \quad D_6 = 0.4 + 0.2\sin(0.2t),$$

and constant coefficients as follows:

$$a_1 = 1.2, \quad a_2 = 0.002, \quad a_3 = -1, \quad a_4 = -0.01, \quad a_5 = 0.02,$$
$$b_1 = 25.4, \quad b_2 = 17.6, \quad b_3 = 23.14, \quad w = 1, \quad m = 1.540, \quad g = 9.81,$$

and consider the desirable trajectories as follows:

$$x_{2d} = e^{-t^2}, \quad x_{4d} = 0.1e^{-2t}, \quad x_{6d} = 0.2e^{-0.01t}, \quad x_{8d} = e^{-t},$$

with the following initial data:

$$(x_1, x_2, x_3, x_4, x_5, x_6) = (0.75, 0.01, 1.02, -0.1, -0.05, -0.05),$$

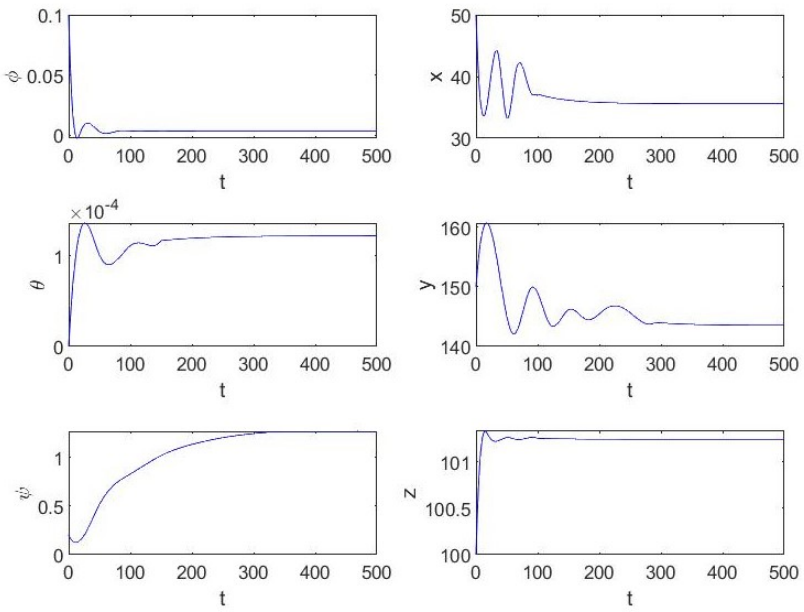

Figure 3: Position of the hexa-rotor in the earth reference frame.

$$(x_7, x_8, x_9, x_{10}, x_{11}, x_{12}) = (200, -0.01, 50, 0.05, 40, 0.1),$$
$$\theta_1 = 1.540, \quad \theta_2 = (0.39, 0.47, -0.000787), \quad \theta_3 = (0.057, 0.057, -0.000568),$$
$$\theta_4 = (0.043, -0.000864).$$

Finally, by applying the adaptive control described in this paper, the trajectory of the roll, pitch, and yaw angles and the trajectory of the position of the hexa-rotor position are shown respectively in Figure 4.

6 Conclusion

In this paper, a nonlinear robust adaptive control strategy based on Lyapunov analysis was developed. The objective of the proposed robust adaptive controller is to reduce the errors of the trajectories by tracking the desired values. The stability of the controlled process, the convergence of the tracking, and bounded parameter adaptation were demonstrated using Lyapunov analysis. The proposed nonlinear robust adaptive control strategy can be used in future works in simulated dynamic systems and realistic health treatments of some patients.

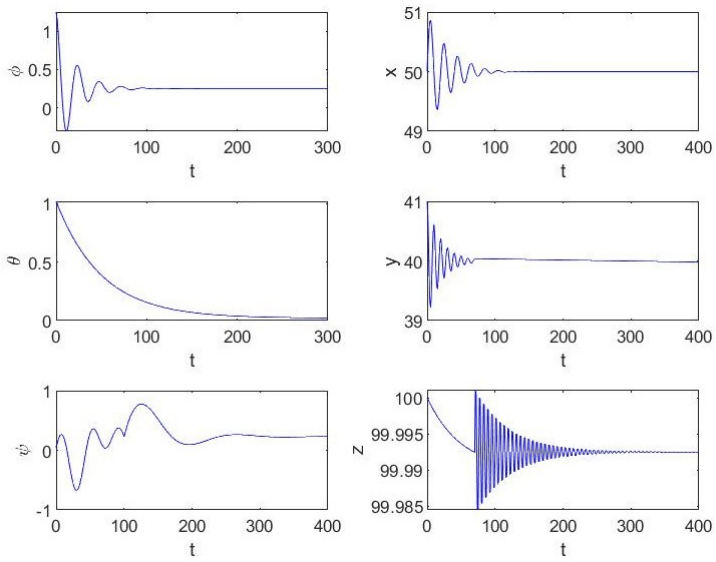

Figure 4: Position of the hexa-rotor in the earth reference frame.

References

[1] Alaimo, A., Artale, V., Milazzo, C., Ricciardello, A., Trefiletti, L. (2013). "Mathematical modeling and control of a hexacopter", In 2013 International Conference on Unmanned Aircraft Systems (ICUAS), 1043-1050.

[2] Ali, R., Peng, Y., Iqbal, M.T., Amin, R.U., Zahid, O., Khan, O.I. (2019). "Adaptive backstepping sliding mode control of coaxial octorotor unmanned aerial vehicle", IEEE Access, 7, 27526-27534.

[3] Analia, R., Song, K.T. (2016). "Fuzzy+ PID attitude control of a co-axial octocopter", In 2016 IEEE International Conference on Industrial Technology (ICIT), IEEE, 1494-1499.

[4] Arellano-Muro, C.A., Luque-Vega, L.F. Castillo-Toledo, B., Loukianov, A.G. (2013). "Backstepping control with sliding mode estimation for a hexacopter", In 2013 10th International Conference on Electrical Engineering, Computing Science and Automatic Control (CCE), IEEE, 31-36.

[5] Artale, V., Milazzo, C.L.R., Ricciardello, A. (2013). "Mathematical modeling of hexacopter", Applied mathematical sciences, 7(97), 4805-4811.

[6] Belmonte, N., Staulo, S., Fiorot, S., Luetto, C., Rizzi, P., Baricco, M. (2018). "Fuel cell powered octocopter for inspection of mobile cranes: Design, cost analysis and environmental impacts", Applied energy, 215, 556-565.

[7] Bouabdallah, S., Siegwart, R. (2005). "Backstepping and sliding-mode techniques applied to an indoor micro quadrotor", In Proceedings of the 2005 IEEE international conference on robotics and automation, 2247-2252.

[8] Chen, Y., Zhang, G., Zhuang, Y., Hu, H. (2019). "Autonomous flight control for multi-rotor UAVs flying at low altitude", IEEE Access, 7, 42614-42625.

[9] Jiao, S., Gao, H., Zheng, X., Liu, D. (2020). "Fault Tolerant Control Algorithm of Hexarotor UAV", Journal of Robotics, 2020, 1-16.

[10] Mahony, R., Kumar, V., Corke, P. (2012). "Multirotor aerial vehicles: Modeling, estimation, and control of quadrotor", IEEE Robotics and Automation magazine, 19(3), 20-32.

[11] Mokhtari, A., Benallegue, A. (2004). "Dynamic feedback controller of Euler angles and wind parameters estimation for a quadrotor unmanned aerial vehicle", In IEEE International Conference on Robotics and Automation, 3, 2359-2366.

[12] Moussid, M., Idalene, A., Sayouti, A., Medromi, H. (2015). "Autonomous hexaRotor arial dynamic modeling and a review of control algorithms", International Research Journal Of Engineering And Technology, 20, 1197-1204.

[13] Nguyen, N.P., Kim, W., Moon, J. (2019). "Super-twisting observer-based sliding mode control with fuzzy variable gains and its applications to fully-actuated hexarotors", Journal of the Franklin Institute, 356(8), 4270-4303.

[14] Rosales, C., Soria, C. M., Rossomando, F.G. (2019). "Identification and adaptive PID Control of a hexacopter UAV based on neural networks", International journal of Adaptive control and signal processing, 33(1), 74-91.

[15] Suicmez, E. C., Kutay, A. T. (2017). "Attitude and altitude tracking of hexacopter via LQR with integral action", In 2017 International Conference on Unmanned Aircraft Systems (ICUAS), 150-159.

[16] Wang, Q., Zhang, H., Han, J. (2018). "Research on trajectory planning and tracking of hexa-copter", In MATEC Web of Conferences, 173.

[17] Wang, Y., Sun, J., He, H., Sun, C. (2019). "Deterministic policy gradient with integral compensator for robust quadrotor control", IEEE Transactions on Systems, Man, and Cybernetics: Systems, 50 (10), 3713-3725.

[18] Wen, F.H., Hsiao, F.Y., Shiau, J.K. (2021). "Analysis and management of motor failures of hexacopter in hover", Actuators, 10, 1-29.

[19] Zhang, J., Gu, D., Deng, C., Wen, B. (2019). "Robust and adaptive backstepping control for hexacopter UAVs", IEEE Access, 7, 163502-163514.

How to Cite this Article:
Zarrabi, M.R. (2022). "Applying Robust Adaptive Lyapunov-Based Control for Hexa-Rotor", Control and Optimization in Applied Mathematics, 7(1): 1-14. doi: 10.30473/COAM.2022.63671.1199